CHEMISTRY
A EUROPEAN JOURNAL

DOI: 10.1002/chem.201000418

The Complexed 1,3-Diphospha-2-Arsaallyl Radical and Its Cationic and Anionic Derivatives

Markus Stubenhofer,[a] Christian Kuntz,[a] Michael Bodensteiner,[a] Ulrich Zenneck,[b] Marek Sierka,[c] and Manfred Scheer*[a]

Dedicated to Professor Wolf-Walther Du Mont on the occasion of his 65th birthday

Abstract: Photolysis of $[Cp^*As\{W(CO)_5\}_2]$ (**1a**) in the presence of Mes*P=PMes* (Mes* = 2,4,6-tri-*tert*-butylphenyl) leads to the novel 1,3-diphospha-2-arsaallyl radical $[(CO)_5W(\mu,\eta^2{:}\eta^1\text{-}P_2AsMes^*_2)W(CO)_4]$ (**2a**). The frontier orbitals of the radical **2a** are indicative of a stable π-allylic system that is only marginally influenced by the d orbitals of the two tungsten atoms. The SOMO and the corresponding spin density distribution of the radical **2a** show that the unpaired electron is preferentially located at the two equivalent terminal phosphorus atoms, which has been confirmed by EPR spectroscopy. The protonated derivative of **2a**, the complex $[(CO)_5W(\mu,\eta^2{:}\eta^1\text{-}P_2As(H)Mes^*_2)W(CO)_4]$ (**6a**) is formed during chromatographic workup, whereas the additional products $[Mes^*P{=}PMes^*\{W(CO)_5\}]$ as the *Z*-isomer (**3**) and the *E*-isomer (**4**), and $[As_2\{W(CO)_5\}_3]$ (**5**) are produced as a result of a decomposition reaction of radical **2a**. Reduction of radical **2a** yields the stable anion $[(CO)_5W(\mu,\eta^2{:}\eta^1\text{-}P_2AsMes^*_2)W(CO)_4]^-$ in **7a**, whereas upon oxidation the corresponding cationic complex $[(CO)_5W(\mu,\eta^2{:}\eta^1\text{-}P_2AsMes^*_2)W(CO)_4][SbF_6]$ (**8a**) is formed, which is only stable at low temperatures in solution. Compounds **2a**, **7a**, and **8a** represent the hitherto elusive complexed redox congeners of the diphospha-arsa-allyl system. The analogous oxidation of the triphosphaallyl radical $[(CO)_5W(\mu,\eta^2{:}\eta^1\text{-}P_3Mes^*_2)W(CO)_4]$ (**2b**) also leads to an allyl cation, which decomposes under CH activation to the phosphine derivative $[(CO)_5W\{\mu,\eta^2{:}\eta^1\text{-}P_3(Mes^*)(C_5H_2tBu_2C(CH_3)_2CH_2)\}W(CO)_4]$ (**9**), in which a CH bond of a methyl group of the Mes* substituent has been activated. All new products have been characterized by NMR spectrometry and IR spectroscopy, and compounds **2a**, **3**, **6a**, **7a**, and **9** by X-ray diffraction analysis.

Keywords: allyl ligands · arsenic · arsenidenes · phosphorus · radicals

Introduction

The allyl radical **A** is a fundamental organic radical that is prominent in both experimental and theoretical organic chemistry.[1–4] As an anion it is an important ligand, just as the amidinato ligand is, which, with bulky substituents at the N atoms, is broadly used to stabilize molecules in unusual bonding situations.[5–10] In contrast, radicals containing group 15 elements formally obtained by an isolobal replacement of CR′ or CR_2 moieties by E and ER, respectively, are rare. An isolable 1,3-diphosphaallyl radical **B** has been synthesized by Bertrand's group,[11a] and another has been observed as a stable side product of a P–C cage rearrangement reaction.[11b] The 2-phosphaallyl radical **C** has only been synthesized in situ by electrochemical reduction of 2-phosphaallyl cations,[12] and its structural parameters have been calculated by quantum chemical methods.[13] Recently, we reported a straightforward synthesis of a novel air-stable

[a] Dipl.-Chem. M. Stubenhofer, Dr. C. Kuntz, Dipl.-Chem. M. Bodensteiner, Prof. Dr. M. Scheer
Institut für Anorganische Chemie der Universität Regensburg
93040 Regensburg (Germany)
Fax: (+49) 941-943-4439
E-mail: manfred.scheer@chemie.uni-regensburg.de

[b] Prof. Dr. U. Zenneck
Department Chemie und Pharmazie and Interdisciplinary Center for Molecular Materials (ICMM), Universität Erlangen-Nürnberg
Egerlandstrasse 1, 91058 Erlangen (Germany)

[c] Dr. M. Sierka
Institut für Chemie der Humboldt-Universität zu Berlin,
10099 Berlin (Germany)

Supporting information for this article is available on the WWW under http://dx.doi.org/10.1002/chem.201000418.

complexed triphosphaallyl radical **D** by photolysis of the Cp*-containing phosphinidene complex [Cp*P{W(CO)$_5$}$_2$] (**1b**)[14] with a diphosphene and its transformation into anionic and cationic derivatives.[15]

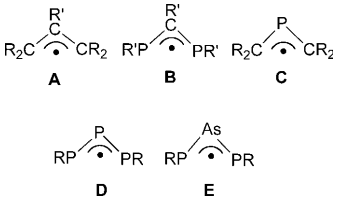

This reactivity pattern of **1b** is unusual, since thermal activation usually leads to a tungsten–phosphorus triple-bond intermediate **F**[16] (Scheme 1), which can be trapped with organometallic compounds containing transition metal multiple bonds,[17] alkynes,[18] and phosphaalkynes[19] to give novel clusters, metal-containing heterocycles, and cage compounds, respectively. Photolysis of **1b** leads to **F** and, additionally, to a radical intermediate **G** by the elimination of a Cp*$^{\bullet}$ moiety.[20] In contrast, for the As homologue [Cp*As{W(CO)$_5$}$_2$] (**1a**) thermolysis yields the triply-bound intermediate **F** along with the radical intermediate **G**, the latter of which is formed exclusively upon photolysis.[21] In continuation of this work, we have turned our attention to investigating how this intermediate acts as an As radical-transfer reagent to a diphosphene to yield an unprecedented type **E** complex. The redox chemistry of the complexed derivative **E** leads to ionic derivatives, and the results of our studies are reported herein.

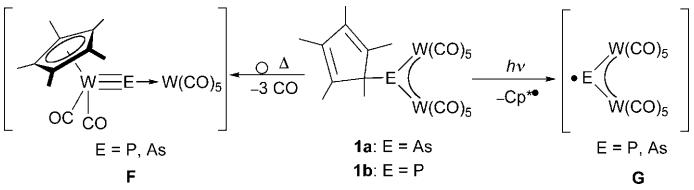

Scheme 1. Different transformation pathways in the photolysis and the thermolysis of the pentelidene complexes **1a**,**b**.

Results and Discussion

Photolysis of [Cp*As{W(CO)$_5$}$_2$] in the presence of Mes*P=PMes* (Mes* = 2,4,6-tri-*tert*-butylphenyl): Photolysis of **1a** in toluene in the presence of Mes*P=PMes* resulted in a color change from deep-blue to greenish-brown after 12 h, which indicated complete transformation of the starting material (Scheme 2). After thin-layer chromatographic workup, the radical [(CO)$_5$W(μ,η^2:η^1-P$_2$AsMes*$_2$)W(CO)$_4$] (**2a**) and the complexes [(CO)$_5$W(μ,η^2:η^1-P$_2$As(H)Mes*$_2$)W(CO)$_4$] (**6a**), [Mes*P=PMes*{W(CO)$_5$}] as the *Z*-isomer (**3**) and *E*-isomer (**4**), and [{W(CO)$_5$}$_3$(μ,η^2-As$_2$)] (**5**) were isolated. Since no thermal reaction takes place between the starting materials (toluene, 110 °C, 2 h), a nucleophilic attack of the diphosphene at the electrophilic arsinidene arsenic atom can be ruled out. Therefore, **2a** is most likely formed by addition of the photogenerated arsenic radical to the P=P double bond followed by a rearrangement. Complex **2a** was isolated as a blackish-green compound in yields of up to 25 %, provided that the formation of **6a** (Scheme 3) was avoided by using specially dried TLC plates. Under these conditions, the ^{31}P NMR spectrum of the reaction mixture showed no signals attributable to **6a**.

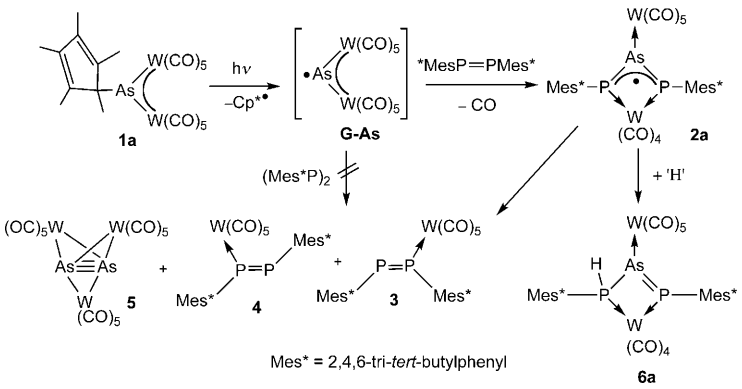

Scheme 2. Reaction pathway for the photolysis of **1a**.

Interestingly, of the isomers **3** and **4**, only the energetically favored *E*-isomer **4** is known.[22] An unusual stereochemistry for bulky Mes* substituents in a *Z*-isomer about a P=P double bond[23] is obtained if the two substituents are coupled in the cyclic carbon core of [{W(CO)$_5$P}$_2$(*t*Bu$_2$C$_6$H$_2$-

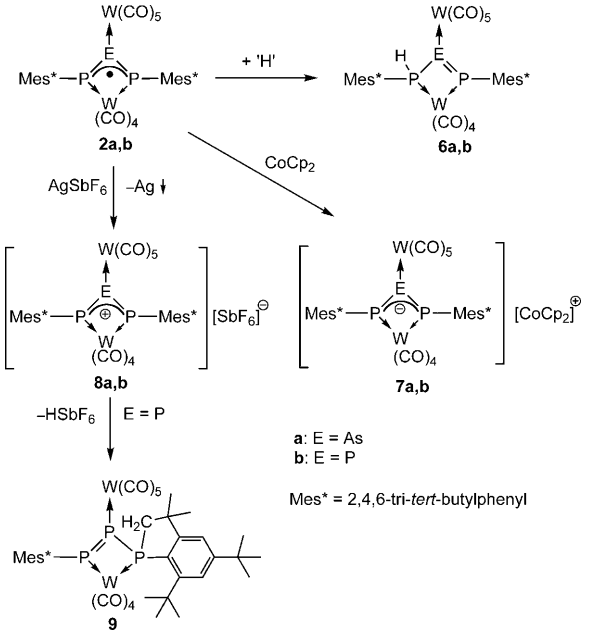

Scheme 3. Oxidation and reduction of the complexed tripentelaallyl radicals.

C_2H_4-$C_6H_2tBu_2$)]. In contrast, if a diphosphene is asymmetrically substituted by Mes* and Mes units, the *Z*-diphosphene complexes [$(CO)_5M(\eta^1$-Mes*P=PMes)] (M = Cr, Mo, W) can be synthesized photochemically from the corresponding *E*-diphosphene complexes. Of these, the Cr derivative has been characterized by X-ray structural analysis.[24] The relatively good yields of the novel symmetrically substituted *Z*-isomer **3** obtained in the present study can most likely be attributed to stereoselective decomposition of the radical **2a**, which leads to initial formation of the *Z*-isomer **3**. Monitoring by ^{31}P NMR spectroscopy revealed that it rearranges over time into the *E*-isomer **4**. Hence, we do not favor the alternative formation pathway of **3** and **4** as $W(CO)_5$-trapping products derived from the decomposition of radical intermediate **G-As** to the As_2 derivative **5**. If this were the case, the initial yield of the *E*-isomer **4** would be much higher.

Compounds **2a** and **6a** were found to be readily soluble in *n*-hexane, toluene, and CH_2Cl_2. The IR spectra of both compounds feature the characteristic absorption pattern of [$W(CO)_5$] groups, and the spectrum of **6a** additionally features a band due to the P–H vibration. The mass spectra feature the corresponding molecular ion peaks. The ^{31}P{H} NMR spectrum of **6a** shows an AX spin system at $\delta = -71.1$ and 423.5 ppm ($^2J_{P,P} = 122$ Hz), with each of the signals displaying a pair of tungsten satellites ($^1J_{P,W} = 203$ Hz, $^1J_{P,W} = 254$ Hz). The signal of the hydrogen-bearing phosphorus atom is shifted upfield, in contrast to that of the phosphorus atom involved in the P=As bond. Both ^{31}P signals appear as doublets of doublets, which may be attributed to P–H coupling ($^1J_{P,H} = 340$ Hz). No NMR signals could be detected for the radical **2a** due to its paramagnetism.

X-band EPR spectroscopy of **2a** revealed characteristic data for a symmetrical 1,3-diphospha-2-arsaallyl radical (Figure 1). The isotropic <g> and <a> (^{31}P) data are in very close agreement with those reported for the two known type **B** PCP allyl radicals, and the observed <a> (^{75}As) value (100%, $I = 3/2$) conforms to the general trends of the theoretical analysis, with smaller and negative spin density at the central allyl nucleus.[11] No trace of a ^{183}W hyperfine interaction could be identified in the spectra. Similar observations have been made for the related P_3 allyl complex radical [$(CO)_5W(\mu,\eta^2{:}\eta^1$-$P_3Mes^*_2)W(CO)_4$] (**2b**).[15]

The remarkable line-broadening of the low-field part of the room temperature spectrum may be attributed to a strong anisotropy of the P and As hyperfine tensors, which were extracted from the glassy frozen solution low-temperature spectrum (Figure 1b). Low-temperature EPR investigations of **2b** resulted in almost identical parameters of $g_1 = 2.069$ and $a_1(1,3\text{-}P_2) = 19.67$ mT,[25] but no low-field hyperfine structure line-broadening effect or significant g- or a-anisotropy has been reported for free radicals **B**.[11] The anisotropy can thus be related to the contributions of the W 5d orbitals to the SOMOs of ditungsten complexes **2**. On the other hand, the close match with the isotropic EPR data of free type **B** radicals and the absence of observable ^{183}W hyperfine interactions points to preferential delocalization of the SOMO predominantly over the central PAsP or PPP allyl units of **2a** and **2b**, respectively.

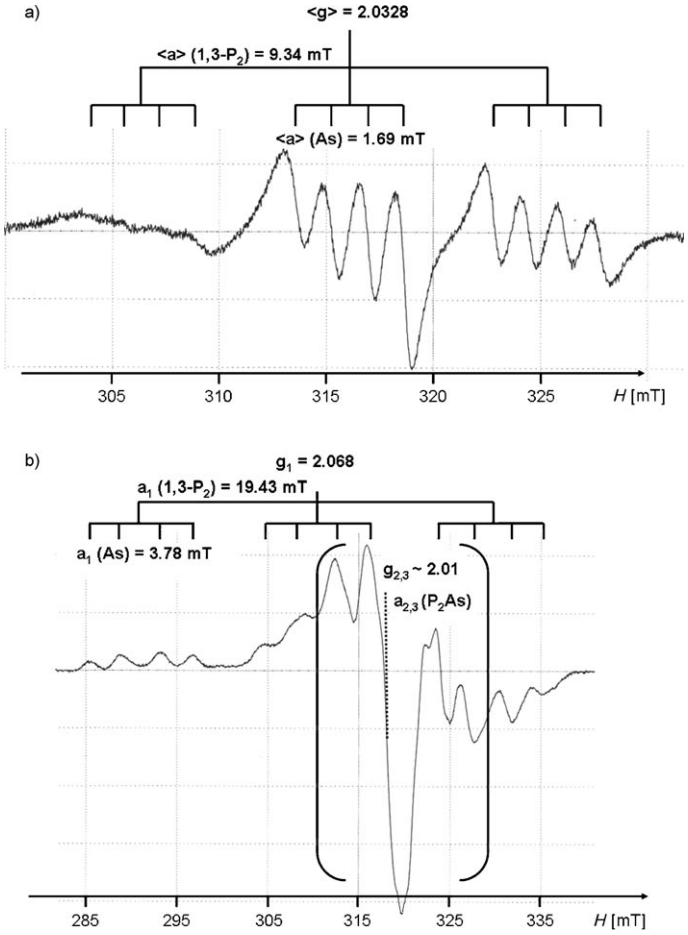

Figure 1. X-band EPR spectra of AsP_2 radical **2a**. a) Liquid solution, 300 K, toluene, 8.988 GHz. b) Glassy frozen solution, 90 K, toluene, 8.988 GHz. Anisotropic EPR data: $g_1 = 2.068$, $g_{2,3} \approx 2.01$; $a_1(1,3\text{-}P_2) = 19.43$ mT, $a_{2,3}(1,3\text{-}P_2) \approx 4.3$ mT; $a_1(As) = 3.78$ mT, $a_{2,3}(As) \approx 0.65$ mT.

Figure 2 shows isosurface plots of the natural π orbitals of the central W2-(η^1)AsP_2(η^2)-W1 unit in **2a**. Not only does the orbital picture closely resemble the classical π system of the C_3 allyl radical, but it is also virtually indistinguishable from that of the triphosphaallyl radical **D** in **2b**.[15] The shape of the SOMO (4a in Figure 2) and the corresponding spin density account for the high spin densities at the terminal P atoms and are consistent with the experimental EPR data. Additionally, the orbital picture also reveals an incorporation of d orbitals of both W atoms within the central AsP_2 allyl moiety. Similar to the situation in the triphosphaallyl radical, the 1b orbital in Figure 2 is a p(As)–d(W2) π-bonding combination. The 2a orbital and SOMO 4a are bonding and antibonding combinations, respectively, of the p(P1/1′) and d(W1) orbitals. The SOMO-1 and LUMO are bonding and antibonding π orbitals of the AsP_2 allyl fragment.

Electrochemical analysis of **2b** showed a reversible one-electron oxidation to the corresponding cation at 0.17 V and

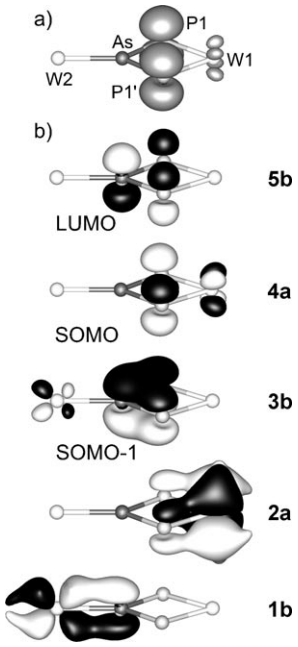

Figure 2. Isosurface plots of a) spin density and b) natural π orbital systems in the ditungsten 1,3-diphospha-2-arsaallyl unit in radical **2a**. The natural orbitals are labeled with their numerical order and symmetry.

a reversible one-electron reduction to the corresponding anion at −0.81 V.[15] Since **2a** readily decomposed into **3** and **5** at ambient temperature, no cyclovoltammetric measurement could be carried out. Therefore, the same reagents as used for **2b** ($AgSbF_6$ and $CoCp_2$)[26] were applied for the oxidation and reduction of **2a** (Scheme 3). The reaction of **2a** with $AgSbF_6$ in CH_2Cl_2 at −78 °C resulted in a rapid color change from greenish-brown to purple, indicating the formation of the cationic compound **8a**. The detected A_2 spin system in the $^{31}P\{H\}$ NMR spectrum shows a singlet at $\delta =$ 376.2 ppm ($^1J_{P,W} = 286$ Hz), revealing the equivalence of the two phosphorus atoms.[27] In solution, this cation is only stable up to 0 °C and monitoring of the decomposition indicated increases in the amounts of $[Mes^*PH_2\{W(CO)_5\}]$[28] and unidentified products. Due to the absence of a proton source, the decomposition product could only have originated from the reaction of **8a** with the solvent CH_2Cl_2. In contrast to the slightly better stability of the oxidation product **8b**,[15] we were unable to isolate **8a** from the reaction mixture due to its rapid decomposition upon warming to room temperature.

Interestingly, when the triphosphaallyl cation **8b**[15,29] was generated from **2b** with $AgSbF_6$ in a similar way as **8a**, only a trace of $[Mes^*PH_2\{W(CO)_5\}]$ was observed as a decomposition product, whereas **9** could be isolated as the main product of this degradation reaction. The formation of **9** can be regarded as originating from an intramolecular electrophilic attack of one of the terminal phosphorus atoms at one of the *ortho-tert*-butyl groups with subsequent elimination of $HSbF_6$. Similar intramolecular CH activations of *tert*-butyl groups of supermesityl substituents have been reported in the literature.[16,30] The $^{31}P\{^1H\}$ NMR spectrum of **9** features three doublets of doublets of an AMX spin system, with each peak showing a pair of tungsten satellites. The signal of the carbon-bearing phosphorus atom is shifted upfield (4.4 ppm) from those of the phosphorus atoms of the P=P double bond ($\delta = 394.8$ and 469.4 ppm). The EI mass spectrum of **9** shows the molecular ion peak at m/z 1202.

The reaction of **2a** with a stoichiometric amount of $CoCp_2$ in CH_2Cl_2 resulted in a color change from greenish-brown to green and the diamagnetic product **7a** could be isolated in 42% yield. The signal of the A_2 spin system at $\delta = 376.2$ ppm in the ^{31}P NMR spectrum of **7a** is shifted upfield with respect to that of the cation **8a** ($\delta = 148.2$ ppm). In comparison to that of **8a** ($^1J_{P,W} = 286$ Hz), the lower value of the $^1J_{P,W}$ coupling constant (160 Hz) indicates a lower s character of the bonds to the tungsten atoms in **7a**. Interestingly, Jutzi et al. have reported spectroscopic evidence for the existence of such an uncomplexed anion.[31]

Crystal structure analysis: Crystallographic data are listed in Table 1. The molecular structure of the greenish-black radical $[(CO)_5W(\mu,\eta^2{:}\eta^1\text{-}P_2AsMes^*_2)W(CO)_4]$ (**2a**) (Figure 3) reveals a Mes*-substituted diphospha-arsa-allylic system, which is coordinated to a $W(CO)_4$ unit through the two "terminal" phosphorus atoms P1 and P1′. The central arsenic atom is coordinated to a $W(CO)_5$ group. The atoms P1, P1′, As1, W1, W2, C6, and C6′ are coplanar. The solid-state structure of **2a** possesses a mirror plane along the atoms W1, As1, and W2, which is orthogonal to the allylic system. The P1–As1 bond length (2.2156(12) Å) is between those of a single bond and a double bond (for the calculated molecule HP=AsH: 2.181 Å).[32] The conjugation of the radical is limited to the P1/P1′/As1/W1/W2 core since the phenyl rings of the Mes* substituents are perpendicular to the allylic system (dihedral angle: 85.06°). At 81.12(5)°, the P1′-As1-P1 angle is in the same range as observed for **2b** (P1′-P2-P1: 83.7(3)°). The W1–P1 and W2–As1 distances (2.463(1) Å and 2.558(1) Å) are in the typical ranges for phosphine and arsine $W(CO)_5$ complexes, respectively.[33]

The molecular structure of **6a** (Figure 4) reveals that protonation of **2a** at P1 distorts the coplanar arrangement of P and W atoms in comparison with the unprotonated **2a**. Subsequently, the P1–As1 bond (2.2981(14) Å) represents a single bond,[34] whereas the As1–P2 bond (2.1787(13) Å) corresponds to a double bond.[35]

X-ray structure analysis of the cobaltocenium salt **7a** (Figure 5) showed the molecule to be only slightly distorted from ideal C_2 symmetry. Deviations from ideal symmetry are most likely due to packing effects in the presence of its counterion in the crystal lattice. In comparison to those in the radical **2a**, the P–As bond lengths are shortened (P1–As1 2.1866(13) Å, As1–P2 2.1907(13) Å) in the anion **7a**, whereas the W<C–P (W1–P1 2.5491(12) Å, W1–P2 2.5644(13) Å, W2–As1 2.5827(4) Å) bond lengths are elongated. Additionally, the coplanar arrangement of the atoms C6, C6′, P1, P1′, P2, W1, and W2 observed in **2a** is distorted in **7a**.

Table 1. Crystallographic data and details of X-ray experiments for **2a**, **3**, **6a**, **7a**, and **9**.

	2a	**3**	**6a**	**7a**	**9**
formula	$C_{45}H_{58}AsO_9P_2W_2$	$C_{41}H_{58}O_5P_2W$	$C_{45}H_{59}AsO_9P_2W_2$	$C_{58}H_{74}AsCl_6CoO_9P_2W_2$	$C_{46}H_{59}Cl_2O_9P_3W_2$
M_r	1247.45	876.65	1248.46	1691.34	1287.43
crystal size [mm]	0.12×0.06×0.04	0.19×0.15×0.12	0.24×0.16×0.05	0.45×0.35×0.11	0.19×0.07×0.05
T [K]	123(1)	123(1)	123(1)	123(1)	123(1)
space group	$C2/c$	$P\bar{1}$	$P\bar{1}$	$P2_1$	$P2_1/n$
crystal system	monoclinic	triclinic	triclinic	monoclinic	monoclinic
a [Å]	15.251(3)	9.5873(2)	9.7503(3)	11.5340(1)	18.542(5)
b [Å]	20.732(4)	10.8710(4)	10.9078(4)	15.6993(2)	11.015(5)
c [Å]	15.836(3)	20.0443(6)	24.5253(8)	18.5095(2)	25.183(5)
α [°]	90	80.744(3)	80.752(3)	90	90
β [°]	94.95(3)	83.601(2)	80.828(3)	90.422(1)	99.614(5)
γ [°]	90	84.600(2)	78.210(3)	90	90
V [Å^3]	4988.4(17)	2042.85(11)	2498.44(15)	3351.53(6)	5071(3)
Z	4	2	2	2	4
ρ_{calcd} [g cm^{-3}]	1.661	1.425	1.660	1.676	1.686
μ [mm^{-1}]	10.141	6.296	10.124	4.495	10.541
radiation ([Å])	$Cu_{K\alpha}$ (1.54178)	$Cu_{K\alpha}$ (1.54178)	$Cu_{K\alpha}$ (1.54178)	$Mo_{K\alpha}$ (0.71073)	$Cu_{K\alpha}$ (1.54178)
diffractometer	Gemini R Ultra	Gemini R Ultra	Gemini R Ultra	Gemini R Ultra	Gemini R Ultra
2θ range [°]	7.22–125.52	4.48–102.90	8.36–130.16	6.20–61.08	5.50–133.30
index range	$-17 \le h \le 17$	$-9 \le h \le 9$	$-10 \le h \le 11$	$-15 \le h \le 16$	$-21 \le h \le 15$
	$-23 \le k \le 16$	$-10 \le k \le 10$	$-12 \le k \le 12$	$-22 \le k \le 22$	$-13 \le k \le 12$
	$-17 \le l \le 18$	$-20 \le l \le 20$	$-28 \le l \le 28$	$-26 \le l \le 26$	$-29 \le l \le 29$
data/restraints/parameters	3954/0/278	4384/0/442	8498/15/563	18026/33/728	8634/7/585
independent reflections	3954	4384	8498	18026	8634
with $I > 2\sigma(I)$	(R_{int}=0.0636)	(R_{int}=0.0282)	(R_{int}=0.0178)	(R_{int}=0.0293)	(R_{int}=0.0242)
GOF in F^2	0.942	1.071	1.068	1.002	1.036
R_1/wR_2 ($I > 2\sigma(I)$)	0.0316, 0.0742	0.0232, 0.0619	0.0314, 0.0718	0.0303, 0.0665	0.0274, 0.0671
R_1/wR_2 (all data)	0.0394, 0.0759	0.0248, 0.0625	0.0344, 0.0734	0.0356, 0.0679	0.0330, 0.0693
largest diff. [e Å^{-3}]	1.159, −0.949	0.755, −0.535	2.957, −1.699	1.500, −1.288	1.954, −0.854

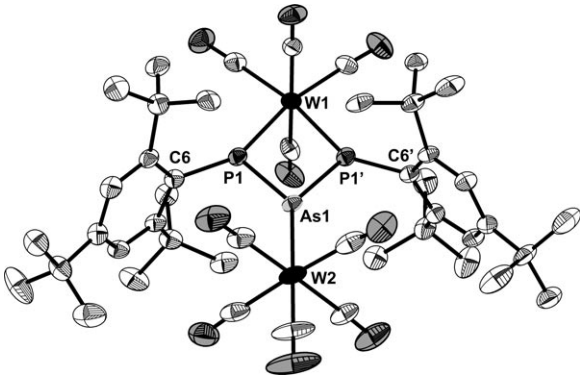

Figure 3. Molecular structure of **2a** in the crystal (50% probability ellipsoids; hydrogen atoms omitted for clarity). Selected bond lengths [Å] and angles [°]: W1–P1 2.4628(12), W2–As1 2.5581(9), As1–P1 2.2156(12), P1–C6 1.833(5); P1′-As1-P1 81.12(5), P1-W1-P1′ 71.60(5), As1-P1-W1 103.64(5), C6-P1-As1 107.86(14), C6-P1-W1 148.34(15).

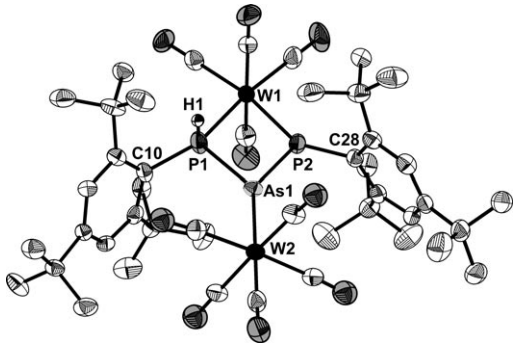

Figure 4. Molecular structure of **6a** in the crystal (50% probability ellipsoids; C-bound hydrogen atoms are omitted for clarity). Selected bond lengths [Å] and angles [°]: W1–P1 2.5179(14), W1–P2 2.4831(12), W2–As1 2.5476(6), As1–P1 2.2981(14), As1–P2 2.1787(13), P1–C10 1.849(5), P2–C28 1.837(5); P1-As1-P2 81.69(5), P1-W1-P2 71.71(4), W1-P1-As1 100.78(5), W1-P2-As1 105.40(5), As1-P1-C10 106.80(16), W1-P1-C10 145.43(15), As1-P2-C28 105.82(15), W1-P2-C28 148.66(16).

The molecular structure of **9** revealed a P_3W_2 frame, in which one of the terminal phosphorus atoms is bound to a C atom of a former methyl group of an *ortho* *t*Bu group (Figure 6). The P1–P2 distance (2.085(27) Å) is in the range for a double bond, whereas at 2.256(6) Å the P2–P3 bond length is in the range for a single bond. The newly formed P3–C35 bond (1.845(10) Å) is comparable to the P–C bonds of the Mes* substituent (P1–C10 1.842(4) Å, P3–C28 1.823(6) Å). The W–P (W1–P1 2.4624(16) Å, W1–P3 2.565(6) Å, W2–P2 2.4505(14) Å) bond lengths are in the same range as in the radical **2b**.

The molecular structure of **3** (Figure 7) shows a Mes*-substituted diphosphene (Figure 5) in the unusual *Z*-configuration. The P–C bond lengths (P1–C6 1.864(3) Å, P2–C24 1.850(3) Å), the P-P-C angles (P2-P1-C6 118.94(10)°, P1-P2-C24 115.05(11)°), and the P–P distance are in the typical ranges for diphosphenes.[23] The torsion angle C6-P1-P2-C24

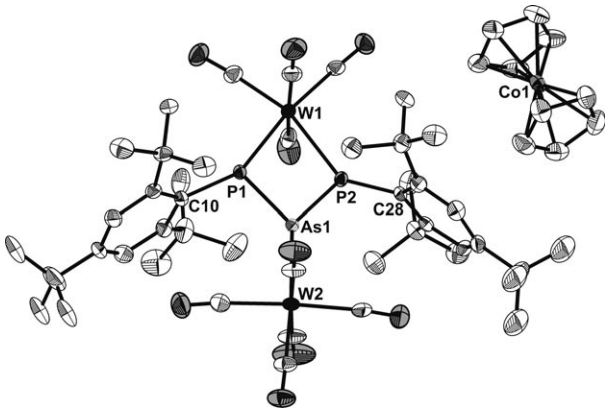

Figure 5. Molecular structure of **7a** in the crystal (50% probability ellipsoids; hydrogen atoms omitted for clarity). Selected bond lengths [Å] and angles [°]: W1−P1 2.5491(12), W1−P2 2.5644(13), W2−As1 2.5827(4), As1−P1 2.1866(13), As1−P2 2.1907(13), P1−C10 1.853(4), P2−C28 1.851(5); P1-As1-P2 86.02(5), P1-W1-P2 71.46(5), W1-P1-As1 101.55(5), W1-P2-As1 100.96(5), As1-P1-C10 110.15(14), W1-P1-C10 140.67(14), As1-P2-C28 108.13(13), W1-P2-C28 143.03(13).

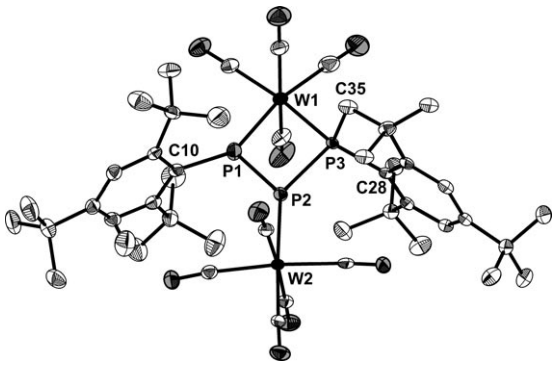

Figure 6. Molecular structure of **9** in the crystal (50% probability ellipsoids; hydrogen atoms omitted for clarity). Selected bond lengths [Å] and angles [°]: W1−P1 2.4624(16), W1−P3 2.565(6), W2−P2 2.4505(14), P1−P2 2.0850(17), P2−P3 2.256(6), P3−C35 1.845(10), P1−C10 1.842(4), P3−C28 1.823(6); P1-P2-P3 85.13(14), P1-W1-P3 71.53(12), W1-P1-P2 104.56(5), W1-P3-P2 96.56(19), P2-P1-C10 110.27(12), W1-P1-C10 144.90(12), P2-P3-C28 104.7(3), W1-P3-C28 143.0(3).

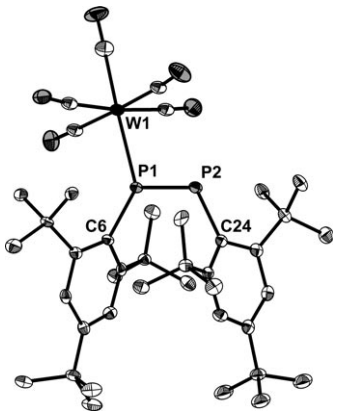

Figure 7. Molecular structure of **3** in the crystal (50% probability ellipsoids; hydrogen atoms omitted for clarity). Selected bond lengths [Å] and angles [°]: P1−P2 2.0502(12), P1−C6 1.864(3), P2−C24 1.850(3), W1−P1 2.5515(9); W1-P1-P2 108.15(4), W1-P1-C6 132.91(10), P2-P1-C6 118.94(10), P1-P2-C24 115.05(11).

is 13.3° due to the high steric requirement of the Mes* groups.

Conclusion

Our results have shown that photolysis of $[Cp^*As\{W(CO)_5\}_2]$ (**1a**) in the presence of Mes*P=PMes* leads to the novel 1,3-diphospha-2-arsaallyl radical **2a**, which is transformed into the protonated derivative $[(CO)_5W(\mu,\eta^2{:}\eta^1\text{-}P_2As(H)Mes^*_2)W(CO)_4]$ (**6a**) upon thin-layer chromatographic workup due to traces of water on the surface of the plates. The radical is less stable than its all-phosphorus congener **2b** and decomposes stereoselectively to the complexes $[Mes^*P{=}PMes^*\{W(CO)_5\}]$ (**3**) as the *Z*-isomer and $[As_2\{W(CO)_5\}_3]$ (**5**). EPR spectroscopy of **2a** has revealed the characteristic features of a heteroallyl radical. The majority of the spin density is symmetrically delocalized over the central PAsP moiety, with dominant contributions from the two terminal phosphorus atoms. The influence of the central arsenic atom is documented by its ^{75}As hyperfine interaction, but the contributions of the two tungsten atoms can only be deduced indirectly from their influence on the anisotropy of the ^{31}P and ^{75}As hyperfine tensors. Reduction of the radical **2a** yields the stable anion in $[Cp_2Co][(CO)_5W(\mu,\eta^2{:}\eta^1\text{-}P_2AsMes^*_2)W(CO)_4]$ (**7a**), whereas upon oxidation with $AgSbF_6$ the corresponding cationic complex $[(CO)_5W(\mu,\eta^2{:}\eta^1\text{-}P_2AsMes^*_2)W(CO)_4][SbF_6]$ (**8a**) is formed, which is only stable at low temperatures in solution. Compounds **2a**, **7a**, and **8a** represent the hitherto elusive complexed redox congeners of the diphospha-arsa-allyl system. Analogous oxidation of $[(CO)_5W(\mu,\eta^2{:}\eta^1\text{-}P_3Mes^*_2)W(CO)_4]$ (**2b**) also leads to an allyl cation, which decomposes under CH activation to a phosphine derivative $[(CO)_5W\{\mu,\eta^2{:}\eta^1\text{-}P_3(Mes^*)(C_5H_2tBu_2C(CH_3)_2CH_2)\}W(CO)_4]$ (**9**). The photochemical generation of As and P radicals of type **G** from the corresponding pentelidene complexes opens up a broad perspective for the synthesis of different As- and P-containing heteroallyl radical systems, making them valuable synthons in main group chemistry.

Experimental Section

General remarks: All reactions were performed under an atmosphere of dry nitrogen using standard vacuum, Schlenk, and glove-box techniques. Solvents were purified and degassed by standard procedures. Commercial grade chemicals were used without further purification. [Mes*P=PMes*],[36] $[Cp^*P\{W(CO)_5\}_2]$,[14,16] and $[Cp^*As\{W(CO)_5\}_2]$[19] were prepared according to literature methods. NMR spectra were recorded at 27°C on a Bruker Avance 400 spectrometer (^1H: 400.132 MHz, standard tetramethylsilane; ^{31}P: 161.976 MHz; standard 85% H_3PO_4; ^{13}C: 100.627 MHz, standard tetramethylsilane). IR spectra were obtained on a Varian FTS 800 spectrometer and mass spectra were recorded on a ThermoQuest Finnigan TSQ 7000 (ESI) or on a Finnigan MAT SSQ 710A (EI). Variable-temperature X-band EPR spectroscopy was performed on a JEOL JES-FA 200 apparatus; standard: Mn^{2+}. Aluminium foil-backed TLC sheets (silica gel 60 F_{254}; Merck) were dried at 100°C for 1 h prior to transferring to a glove box for thin-layer chromatographic workup.

Photolysis of [Cp*As{W(CO)$_5$}$_2$] (1a) in the presence of Mes*P=PMes*: A solution of Mes*P=PMes* (195 mg, 0.35 mmol) in toluene (50 mL) was added to a solution of [Cp*As{W(CO)$_5$}$_2$] (**1a**) (300 mg, 0.35 mmol) in toluene (50 mL). The mixture was irradiated through quartz glass with light from a mercury lamp and was stirred for 2 h at 15 °C, during which time the color of the solution changed from deep-blue to greenish-brown. After removal of all volatile compounds in vacuum, the residue was separated by thin-layer chromatography (hexane/dichloromethane, 3:1) in a glove box. The compounds **3/4** (yellow fraction, 115 mg, 0.13 mmol, 40 %, main product **3**), **2a** (blackish-green fraction, 65 mg, 0.05 mmol, 15 %), and **6a** (blue fraction, 103 mg, 0.08 mmol, 23 %) were isolated. Crystals of **2a**, **3**, and **6a** suitable for X-ray analysis were obtained from solutions in CH_2Cl_2 at −25 °C.

2a: IR (toluene): $\tilde{\nu}$ = 2074 (m), 2023 (s), 1996 (w), 1958 (vs), 1942 (vs), 1915 cm^{-1} (m); MS (EI): *m*/*z* (%): 1248 (60) [M^++H], 1163 (40) [M^++H−3CO], 1136 (5) [M^++H−4CO]; EPR (300 K, toluene, 8.988 GHz): g = 2.0328, a(^{31}P) = 9.34 mT (2P), a(^{75}As) = 1.69 mT; (90 K, toluene, 8.988 GHz): g_1 = 2.008, $g_{2,3} \approx$ 2.04; a_1(2P) = 19.43 mT, $a_{2,3}$(2P) ≈ 4.3 mT; a_1(As) = 3.78 mT, $a_{2,3}$(As) ≈ 0.65 mT.

3: ^{31}P{H} NMR (161.976 MHz, CD_2Cl_2): δ = 307.6 (d, $^1J_{P,P}$ = 569 Hz, $^1J_{P,W}$ = 252 Hz), 392.2 ppm (d, $^1J_{P,P}$ = 569 Hz).

4: ^{31}P{H} NMR (161.976 MHz, CD_2Cl_2): δ = 375.6 (d, $^1J_{P,P}$ = 562 Hz, $^1J_{P,W}$ = 250 Hz), 465.3 ppm (d, $^1J_{P,P}$ = 562 Hz).

6a: IR (KBr): $\tilde{\nu}$ = 2361 (w), 2074 (m), 2019 (vs), 1998 (w), 1969 (vs), 1940 (s), 1920 (s), 1909 cm^{-1} (m); ^{1}H NMR (400.13 MHz, CD_2Cl_2): δ = 1.30 (s, 9H; *p*-*t*Bu), 1.32 (s, 9H; *p*-*t*Bu), 1.66 (s, 9H; *o*-*t*Bu), 1.67 (s, 9H; *o*-*t*Bu), 1.67 (s, 9H; *o*-*t*Bu), 1.68 (s, 9H; *o*-*t*Bu), 7.23 (dd, $^1J_{H,P}$ = 340 Hz, $^3J_{H,P}$ = 19 Hz, 1H; PH), 7.36–7.48 ppm (m, 4H; Ph-H); ^{31}P{^{1}H} NMR (161.976 MHz, CD_2Cl_2): δ = −71.1 (d, $^2J_{P,P}$ = 122 Hz, $^1J_{P,W}$ = 203 Hz), 423.5 ppm (d, $^2J_{P,P}$ = 122 Hz, $^1J_{P,W}$ = 254 Hz); ^{31}P NMR (161.976 MHz, CD_2Cl_2): δ = −71.1 (dd, $^2J_{P,P}$ = 122 Hz, $^1J_{P,H}$ = 340 Hz), 423.5 ppm (dd, $^2J_{P,P}$ = 122 Hz, $^3J_{P,H}$ = 19 Hz); MS (EI): *m*/*z* (%): 1248 (20) [M^+], 1108 (5) [M^+−5CO], 1024 (7) [M^+−8CO], 996 (12) [M^+−9CO].

Reduction of 2a with CoCp$_2$: A solution of $CoCp_2$ (10 mg, 0.05 mmol) in CH_2Cl_2 (5 mL) was added to a solution of **2a** (67 mg, 0.05 mmol) in CH_2Cl_2 (10 mL) at −78 °C. The color of the solution immediately changed from blackish-green to green. Crystals of **7a** (30 mg, 42 %) suitable for X-ray structure analysis were obtained from the concentrated reaction mixture at −25 °C. **7a**: IR (KBr): $\tilde{\nu}$ = 2067 (m), 2020 (w), 1998 (s), 1931 (vs), 1891 (s), 1858 cm^{-1} (sh); ^{1}H NMR (400.13 MHz, CD_2Cl_2): δ = 1.30 (s, 18H; *p*-*t*Bu), 1.71 (s, 36H; *o*-*t*Bu), 5.63 (s, 10H; Cp), 7.29 ppm (s, 4H; Ph-H); ^{31}P{^{1}H} NMR (161.976 MHz, CD_2Cl_2, 273 K): δ = 148.2 ppm (s, $^1J_{P,W}$ = 160 Hz); ^{31}P NMR (161.976 MHz, CD_2Cl_2, 273 K): δ = 148.2 ppm (s, $^1J_{P,W}$ = 160 Hz); MS (ESI): *m*/*z* (%): 188.9 (100) [KCoCp$_2^+$], 1247.2 (100) [A(CO)$_5$W(μ,η^2:η^1-P$_2$AsMes*$_2$)W(CO)$_4^-$].

Oxidation of 2a with AgSbF$_6$: A solution of $AgSbF_6$ (16 mg, 0.04 mmol) in CH_2Cl_2 (5 mL) was added to a solution of **2a** (56 mg, 0.04 mmol) in CH_2Cl_2 (10 mL) at −78 °C. The color of the mixture immediately changed from blackish-green to purple and a silver mirror was formed. The product **8a** was found to be stable only at low temperatures, and so was immediately characterized by ^{31}P{H} NMR spectrometry at −40 °C. After 30 min at 25 °C, **8a** decomposed to {Mes*PH$_2$[W(CO)$_5$]} and further unidentified products. **8a**: ^{31}P{^{1}H} NMR (161.976 MHz, CD_2Cl_2): δ = 376.2 ppm (s, $^1J_{P,W}$ = 286 Hz).

Oxidation of 2b with AgSbF$_6$: A solution of $AgSbF_6$ (16 mg, 0.04 mmol) in CH_2Cl_2 (5 mL) was added to a solution of **2b** (54 mg, 0.04 mmol) in CH_2Cl_2 (10 mL) at −78 °C. The color of the mixture immediately changed from blackish-green to purple and a silver mirror was formed. The product **8b** was found to be stable only at low temperatures, and so was immediately characterized by ^{31}P{H} NMR spectrometry at −40 °C. After 30 min at 25 °C, the color changed from purple to green, indicating the formation of **9**. Crystals of **9** (20 mg, 41 %) suitable for X-ray structure analysis were obtained from the concentrated reaction mixture at −25 °C.

8b: ^{31}P{^{1}H} NMR (161.976 MHz, CD_2Cl_2): δ = 586.5 (t, $^1J_{P,P}$ = 250 Hz, $^1J_{P,W}$ = 272 Hz; P_A), 344.5 ppm (d, $^1J_{P,P}$ = 250 Hz, $^1J_{P,W}$ = 267 Hz; P_M).

9: IR (CH_2Cl_2): $\tilde{\nu}$ = 2071 (m), 2021 (s), 1959 (vs), 1942 (sh), 1903 cm^{-1} (sh); ^{31}P{^{1}H} NMR (161.976 MHz, CD_2Cl_2): δ = 4.4 (dd, $^1J_{P,P}$ = 130 Hz, $^2J_{P,P}$ = 117 Hz, $^1J_{P,W}$ = 206 Hz), 394.8 (dd, $^1J_{P,P}$ = 287 Hz, $^2J_{P,P}$ = 117 Hz, $^1J_{P,W}$ = 217 Hz), 469.4 ppm (dd, $^1J_{P,P}$ = 287 Hz, $^2J_{P,P}$ = 130 Hz, $^1J_{P,W}$ = 232 Hz); MS (EI): *m*/*z* (%): 1202 (32) [M^+].

Crystal structure analysis: Machine parameters, crystal data, and data collection parameters are summarized in Table 1. Crystal structure analyses were performed on an Oxford Diffraction Gemini R Ultra CCD. Semi-empirical absorption corrections from equivalents (multi-scan) were applied for **2a** and **3**.[37] For **6a**, **7a**, and **9** analytical absorption corrections from crystal faces were applied.[38] The structures were solved by direct methods with the program SIR-97,[39] and full-matrix least-squares refinement on F^2 was performed with SHELXL-97[40] with anisotropic displacements for non-H atoms. Hydrogen atoms were placed in idealized positions and refined isotropically according to a riding model. In **3**, **6a**, **7a**, and **9**, the *trans-tert*-butyl groups are disordered over two positions. Additionally, **7a** has disordered phosphorus positions and **9** represents a mixed crystal with 50 % occupancy of each site, corresponding to the ionic and covalent forms of the P3(A)-C35(A) contact. Thus, several constraints and restraints had to been used for the refinement.

CCDC-760727 (**2a**), 760728 (**3**), 760729 (**6a**), 760730 (**7a**), and 760731 (**9**) contain the supplementary crystallographic data for this paper. These data can be obtained free of charge from The Cambridge Crystallographic Data Centre via www.ccdc.cam.ac.uk/data_request/cif

Theoretical calculations: All calculations were performed using the TURBOMOLE program package.[41] The BP86 exchange-correlation functional[42] was used with the triple-zeta plus polarization (TZVP) basis sets on all atoms.[43] To speed up the calculations, the Coulomb part was evaluated using the MARI-J method[44] with optimized auxiliary basis sets on all atoms.[45] Quasi-relativistic pseudopotentials were used for W.[46]

Acknowledgements

This work was comprehensively supported by the Deutsche Forschungsgemeinschaft and the Fonds der Chemischen Industrie. The authors are grateful to COST action CM0802 (PhoSciNet) for general support. M.S. gratefully acknowledges Prof. Joachim Sauer and the Humboldt-Universität zu Berlin for providing computing facilities.

[1] M. J. Plater, S. Kemp, E. Lattmann, *J. Chem. Soc. Perkin Trans. 1* **2000**, 971–979.
[2] B. Giese, W. Damm, R. Batra, *Chemtracts: Org. Chem.* **1994**, *7*, 355–370.
[3] S. G. DiMagno, K. C. Waterman, D. V. Speer, A. Streitwieser, *J. Am. Chem. Soc.* **1991**, *113*, 4679–4681.
[4] N. Azuma, T. Ozawa, J. Yamauchi, *Bull. Chem. Soc. Jpn.* **1994**, *67*, 31–38.
[5] F. T. Edelmann, *Coord. Chem. Rev.* **1994**, *137*, 403–481, and references therein.
[6] J. Barker, M. Kilner, *Coord. Chem. Rev.* **1994**, *133*, 219–300, and references therein.
[7] E. A. C. Brussee, A. Meetsma, B. Hessen, J. H. Teuben, *Organometallics* **1998**, *17*, 4090–4095.
[8] a) M. P. Coles, *J. Chem. Soc. Dalton Trans.* **2006**, 985–1001; b) P. J. Stewart, A. J. Blake, P. J. Mountford, *Inorg. Chem.* **1997**, *36*, 1982–1986.
[9] a) N. Thirupathi, G. P. A. Yap, D. S. Richeson, *Organometallics* **2000**, *19*, 2573–2579; b) K. Albahily, E. Koc, D. Al-Baldawi, D. Savard, S. Gambarotta, T. J. Burchell, R. Duchateau, *Angew. Chem.* **2008**, *120*, 5900–5903; *Angew. Chem. Int. Ed.* **2008**, *47*, 5816–5819; c) S. P. Green, C. Jones, A. Stasch, *Science* **2007**, *318*, 1754–1757.
[10] S. Nagendran, H. W. Roesky, *Organometallics* **2008**, *27*, 457–492.
[11] a) Y. Canac, A. Baceiredo, W. W. Schöller, D. Gigmes, G. Bertrand, *J. Am. Chem. Soc.* **1997**, *119*, 7579–7580; b) M. M. Al-Ktaifani, W. Bauer, U. Bergsträßer, B. Breit, M. D. Francis, F. W. Heinemann,

P. B. Hitchcock, A. Mack, J. F. Nixon, H. Pritzkow, M. Regitz, M. Zeller, U. Zenneck, *Chem. Eur. J.* **2002**, *8*, 2622–2633.
[12] a) A. Schmidpeter, S. Lochschmidt, A. Willhalm, *Angew. Chem.* **1983**, *95*, 561–562; *Angew. Chem. Int. Ed. Engl.* **1983**, *22*, 545–546; b) A. Schmidpeter, A. Willhalm, J. Kroner, R. O. Day, J. M. Holmes, R. E. Holms, *Phosphorus Sulfur Relat. Elem.* **1987**, *30*, 495–498.
[13] W. W. Schoeller, W. Haug, J. Strutwolf, T. Busch, *J. Chem. Soc. Faraday Trans.* **1996**, *92*, 1751–1755.
[14] a) R. Kroos, Ph.D. thesis, Universität Bielefeld (Germany), **1989**; b) P. Jutzi, R. Kroos, *J. Organomet. Chem.* **1990**, *390*, 317–322.
[15] M. Scheer, C. Kuntz, M. Stubenhofer, M. Linseis, R. Winter, M. Sierka, *Angew. Chem.* **2009**, *121*, 2638–2642; *Angew. Chem. Int. Ed.* **2009**, *48*, 2600–2604.
[16] M. Scheer, E. Leiner, P. Kramkowski, M. Schiffer, G. Baum, *Chem. Eur. J.* **1998**, *4*, 1917–1923.
[17] M. Scheer, D. Himmel, C. Kuntz, S. Zhan, E. Leiner, *Chem. Eur. J.* **2008**, *14*, 9020–9029.
[18] a) M. Schiffer, M. Scheer, *Chem. Eur. J.* **2001**, *7*, 1855–1861; b) M. Schiffer, M. Scheer, *J. Chem. Soc. Dalton Trans.* **2000**, 2493–2494; for reviews, see: B. P. Johnson, G. Balázs, M. Scheer, *Coord. Chem. Rev.* **2006**, *250*, 1178–1195; G. Balázs, L. Gregoriades, M. Scheer, *Organometallics* **2007**, *26*, 3058–3075.
[19] M. Scheer, D. Himmel, B. P. Johnson, C. Kuntz, M. Schiffer, *Angew. Chem.* **2007**, *119*, 4045–4049; *Angew. Chem. Int. Ed.* **2007**, *46*, 3971–3975.
[20] M. Schiffer, E. Leiner, M. Scheer, *Eur. J. Inorg. Chem.* **2001**, 1661–1663.
[21] B. P. Johnson, M. Schiffer, M. Scheer, *Organometallics* **2000**, *19*, 3404–3409.
[22] M. Yoshifuji, N. Shinohara, K. Toyota, *Tetrahedron Lett.* **1996**, *37*, 7815–7818.
[23] L. Weber, *Chem. Rev.* **1992**, *92*, 1839–1906.
[24] M. Yoshifuji, T. Hashida, N. Inamoto, K. Hirotsu, T. Higuchi, K. Ito, S. Nagase, *Angew. Chem.* **1985**, *97*, 230–231; *Angew. Chem. Int. Ed. Engl.* **1985**, *24*, 211–212.
[25] See the Supporting Information.
[26] N. G. Connelly, W. E. Geiger, *Chem. Rev.* **1996**, *96*, 877–910.
[27] For 1,3-diphospha-2-arsa cationic systems with λ^5-phosphorane P atoms, see: a) B. D. Ellis, M. Carlesimo, C. L. B. Macdonald, *Chem. Commun.* **2003**, 1946–1947; b) H. Ackermann, J. Aust, M. Driess, K. Merz, C. Monsé, C. von Wüllen, *Phosphorus Sulfur Relat. Elem.* **2002**, *177*, 1613–1617; c) M. Driess, H. Ackermann, J. Aust, K. Merz, C. von Wüllen, *Angew. Chem.* **2002**, *114*, 467–470; *Angew. Chem. Int. Ed.* **2002**, *41*, 450–453.
[28] M. Yoshifuji, T. Hashida, K. Shibayama, N. Inamoto, *Chem. Lett.* **1985**, 287–290.
[29] M. Scheer, C. Runtz, M. Stubenhofer, M. Zabel, A. Y. Timoshkiu, *Angew.Chem.* **2010**, *122*, 192–196; *Angew. Chem. Int. Ed.* **2010**, *49*, 188–192.
[30] A. Cowley, J. Kilduff, N. Norman, M. Paluski, *J. Am. Chem. Soc.* **1983**, *105*, 4845–4846.
[31] P. Jutzi, U. Meyer, *Phosphorus Sulfur Relat. Elem.* **1988**, *40*, 275–277; for a cyclic anionic system, see: R. Edge, R. J. Less, V. Naseri, E. J. L. McInnes, R. E. Mulvey, D. S. Wright, *Dalton Trans.* **2008**, 6454–6460.
[32] L. Mahe, J.-C. Barthelat, *J. Phys. Chem.* **1995**, *99*, 6819–6827.
[33] U. Vogel, M. Scheer, *Z. Anorg. Allg. Chem.* **2001**, *627*, 1593–1598.
[34] M. Stubenhofer, C. Kuntz, G. Balazs, M. Zabel, M. Scheer, *Chem. Commun.* **2009**, 1745–1747.
[35] M. Bouslikhane, H. Gornitzka, J. Escudié, H. Ranaivonjatovo, *J. Organomet. Chem.* **2001**, *619*, 275–279.
[36] M. Yoshifuji, I. Shima, N. Inamoto, K. Hirotsu, T. Higuchi, *J. Am. Chem. Soc.* **1981**, *103*, 4587–4589.
[37] CrysAlis RED, Version 1.171.30.3, Oxford Diffraction Ltd., **2006**.
[38] R. C. Clark, J. S. Reid, *Acta Crystallogr. Sect. A* **1995**, *51*, 887–897.
[39] A. Altomare, M. C. Burla, M. Camalli, G. L. Cascarano, C. Giacovazzo, A. Guagliardi, A. G. G. Moliterni, G. Polidori, R. Spagna, *J. Appl. Crystallogr.* **1999**, *32*, 115–119.
[40] G. M. Sheldrick, *Acta Crystallogr. Sect. A* **2008**, *64*, 112–122.
[41] a) TURBOMOLE V6.0 2009, a development of University of Karlsruhe and Forschungszentrum Karlsruhe GmbH, 1989–2007, TURBOMOLE GmbH, since 2007; available from http://www.turbomole.com; b) R. Ahlrichs, M. Bär, M. Häser, H. Horn, C. Kölmel, *Chem. Phys. Lett.* **1989**, *162*, 165–169; c) O. Treutler, R. Ahlrichs, *J. Chem. Phys.* **1995**, *102*, 346–354.
[42] a) A. D. Becke, *Phys. Rev. A* **1988**, *38*, 3098–3100; b) S. H. Vosko, L. Wilk, M. Nusair, *Can. J. Phys.* **1980**, *58*, 1200–1211; c) J. P. Perdew, *Phys. Rev. B* **1986**, *33*, 8822–8824; erratum: J. P. Perdew, *Phys. Rev. B* **1986**, *34*, 7406.
[43] F. Weigend, R. Ahlrichs, *Phys. Chem. Chem. Phys.* **2005**, *7*, 3297–3305.
[44] K. Eichkorn, O. Treutler, H. Öhm, M. Häser, R. Ahlrichs, *Chem. Phys. Lett.* **1995**, *242*, 652–660; M. Sierka, A. Hogekamp, R. Ahlrichs, *J. Chem. Phys.* **2003**, *118*, 9136–9148.
[45] F. Weigend, *Phys. Chem. Chem. Phys.* **2006**, *8*, 1057–1065.
[46] D. Andrae, U. Häußermann, M. Dolg, H. Stoll, H. Preuß, *Theor. Chim. Acta* **1990**, *77*, 123–141.

Received: February 16, 2010
Published online: May 19, 2010

